

# Development of Innovative Diesel Particulate Filters based on Aluminum Titanate: Design and Validation

Sumitomo Chemical Co., Ltd.

Basic Chemicals Research Laboratory

Akiyoshi NEMOTO

Kentaro IWASAKI

Osamu YAMANISHI

Kazuya TSUCHIMOTO

Kousuke UOE

Tetsuro TOMA

Hajime YOSHINO

Diesel particulate filters have contributed to decreasing particulate matter (PM) in the exhaust gas of diesel cars, and they have become standard diesel exhaust gas after-treatment devices. Silicon carbide (SiC) is currently used as a material in these filters due to its high thermal stability. Aluminum titanate (AT) is recognized as a candidate for the next generation of filters due to advantages not only in manufacturing cost but also in superior performance.

We have developed an innovative AT filter, and in this paper we introduce its design concepts and validation results.

This paper is translated from R&D Report, "SUMITOMO KAGAKU", vol. 2011-II.

## Introduction

In order to halt the progress of global warming, attention has been increasingly given to technologies for reducing carbon dioxide (CO<sub>2</sub>) emissions, and the reduction of CO<sub>2</sub> discharged from automobiles has garnered a lot of interest. It is considered that for the next two decades the internal combustion engine will be an appropriate selection as a power train for automobiles. Especially, diesel-powered automobiles have better fuel efficiency than gasoline-fueled automobiles, and thus they are recognized part of the "eco-car" category. However, it is crucial to implement environmental measures for diesel-powered automobiles also, including the reduction of particulate matter (PM) and nitrogen oxide (NO<sub>x</sub>) discharged from diesel engines. As part of these environmental measures, studies of the exhaust gas after-treatment systems for diesel engines have been actively conducted for quite some time, mainly in Europe and America. Particularly for the PM issue, the adoption of diesel particulate filters (hereinafter referred to as "DPF") has enabled us to obtain certain prospective solutions.<sup>1)</sup> However, as is typically seen in Europe, regulations have been more and more stringent (Table 1)<sup>2)</sup>, and thus development of higher-performance DPFs is even now being undertaken.

**Table 1** European regulations on diesel passenger cars

	Euro5	Euro6
Phase-in Dates	Sep 1, 2009	Sep 1, 2014
PM	5mg/km	4.5mg/km
NO <sub>x</sub>	180mg/km	80mg/km

A wall-flow type filter structure is mainly used in DPFs. This type of filter is now mainly made from ceramics, and the inlet and outlet of the honeycomb structure are alternately plugged, and the honeycomb wall face is used as a filtration area. The honeycomb wall has a porous structure, and PM is removed from the exhaust gases as it passes through this porous layer (Fig. 1). However, it is said that the fuel efficiency will be worse by 1% to 3% once a DPF is installed because the exhaust gas pressure loss will be higher due to the PM accumulation on the DPF, and PM accumulation on the DPF must be periodically burned and removed.<sup>3)</sup>

Currently, silicon carbide (SiC) having outstanding heat resistance properties is the principal material used for DPFs. Because SiC has a high coefficient of thermal expansion, a "segment" type is utilized in SiC DPFs. With this type, prismatic-shaped basic units with spe-

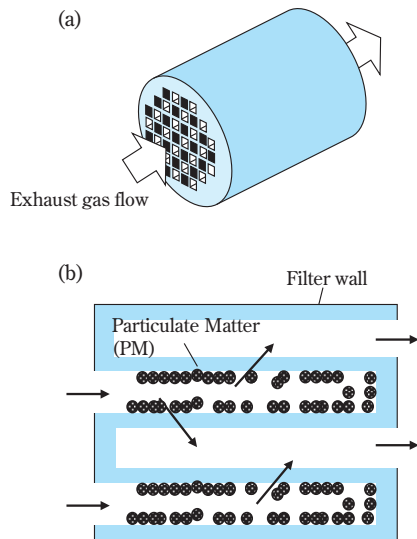


**Fig. 1** (a) Diesel particulate filter (DPF) and (b) PM filtration mechanism by “wall-through” structure observed from cross-section area.

cific dimensions are bonded to each other, and the thermal expansion of the whole DPF is absorbed by the conjugation layers (Fig. 2 (a)). However, because the manufacturing cost for segment-type DPFs is high and material loss is significant as compared to “monolith” type DPFs, it is one of the high cost factors for DPFs. Furthermore, it also has a disadvantage in terms of performance in that the conjugation layers may become “dead space” that does not function in PM removal.

Directing attention to aluminum titanate (AT), which possesses high thermal stability and low thermal

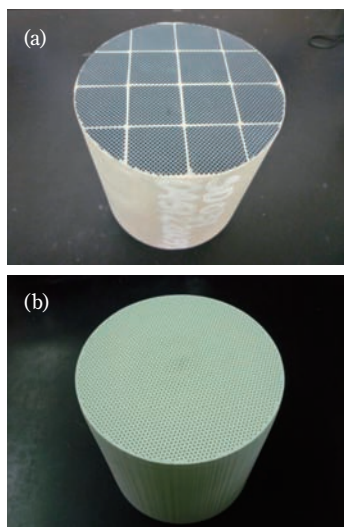


**Fig. 2** Photos of basic filter structure (a) SiC (segment-binding structure) and (b) SC-AT (monolith structure).

expansion properties, we have been engaged in the development of a next-generation DPF in which a monolith can be utilized, and which exceeds the filter properties of the on-market DPFs (Fig. 2 (b)). In this paper the basic design concepts of the DPF we have developed is explained. We have also validated the product design through the evaluation of the DPF manufactured on the basic design concept, and thus offer the following report.

## DPF Product Development Method

The DPF product development method undertaken at Sumitomo Chemical is explained below:

The fact that other companies have already formed the DPF market makes Sumitomo Chemical, so to speak, a “latecomer” manufacturer. Aiming to enter into the DPF market during the Euro6 regulation implementation year (2014), we have been engaged in product development on the major premise of developing a DPF having higher functionality but a lower cost than that of the on-market DPFs within a short period of time at a level of mass-production quality which is in accordance with the international standards of the quality management systems for the automotive industry (ISO/TS16949).

The typical required properties of the DPF summarized from the results of market surveys and customer information are as follows:

- (i) Pressure drop characteristics
- (ii) PM collection characteristics (filtration efficiency)
- (iii) Thermal stability characteristics
- (iv) Thermal shock resistance characteristics
- (v) Mechanical strength characteristics (initial, repeated)
- (vi) Ash-resistance characteristics (physical accumulation amount, reactivity with base material)

Although the level of each requirement varies depending on the customer, the product design was verified by comparing the performance of our DPF to that of the on-market DPF.

## DPF Basic Design Concept

DPF design items consist of the following factors:

- (i) Material design: Design for a DPF material. This will affect the DPF thermal stability, thermal shock resistance, mechanical strength and ash-resistance characteristics (reactivity with the base material).

- (ii) Pore structure design: Design for the pore characteristics of the wall used as a filtration area. This will affect the filter's basic properties, namely the pressure drop characteristics and filtration efficiency.
- (iii) Cell structure design: Design for the honeycomb cell structure (configuration). This will affect the pressure drop, thermal shock resistance and ash-resistance characteristics (physical accumulation).
- (iv) Macro design: Design for the DPF dimensions and configuration. The customer will specify this in consideration of canning and loading characteristics.

The summarized design concept for (i), (ii) and (iii) will be described below:

### 1. Material Design

The parts used for vehicle emission gas lines are exposed to various harsh conditions. For example, severe thermal history due to sudden changes in the engine operating status, vibrations from the engine and road surface, and coming into contact with chemical compositions such as ash having high reactivity and originating from fuel or oil.

Above all, when using a DPF, the PM collected inside the filter must be burned and removed after accumulating for a certain period of time (this process will be hereinafter referred to as "regeneration"). The combustion heat generated during this process will cause the DPF to be exposed to a more severe thermal history than any other part. Although DPF regeneration is normally conducted under relatively mild and controlled conditions, on rare occasions it is performed under an uncontrollable condition (we call this type of regeneration "worst-case regeneration"). Under such conditions, the greater the PM amount is, the more severe the combustion will be. Therefore, the regeneration start timing is set according to actual vehicles so as not to damage filters. This regeneration start timing is determined based on the SML value obtained from a Soot Mass Limit (SML) test, which will be described in the last half of this paper. The larger the SML value is,

the greater is the PM amount that can be burned and removed at once, thus causing regeneration to occur less frequently, thereby improving the fuel efficiency.

The thermal shock parameter (TSP) and heat capacity of a base material can be considered as factors that would affect the SML value. The TSP can be simply calculated as a correlation equation of material properties as shown below:<sup>4)</sup> Regarding MOR/eMod in this equation, since values usually fluctuate in sync with each other and the MOR/eMod ratio is nearly a constant value, it is assumed that reducing the coefficient of thermal expansion (CTE) is most effective to improve the TSP.

$$TSP = MOR / (CTE \times eMod) \quad (1)$$

TSP ; Thermal shock parameter

MOR ; Bending strength

eMod; Young modulus

CTE ; Coefficient of thermal expansion

Furthermore, the heat capacity of the DPF can be considered as a material property that directly contributes to the SML. The temperature of the DPF itself will increase due to the heat generated during the DPF regeneration. The larger the heat capacity is, the milder the heating behavior will be during the regeneration (= sudden temperature change is minimal). When comparing ceramic materials having identical volume, "the material density is large" can be rephrased as "the heat capacity is large."

The material properties of the existing DPF materials, which are SiC and cordierite ( $2Al_2O_3 \cdot 2MgO \cdot 5SiO_2$ ), and aluminum titanite developed by Sumitomo Chemical (hereinafter referred to as "SC-AT") are shown in **Table 2**. Because SC-AT possesses a low CTE and a high heat capacity, favorable SML properties can be expected. It can therefore be considered that SC-AT is more suitable than the existing materials for use in DPF. However, because AT is located in the region of metastable phase at a temperature ranging from 1000°C to 1200°C, it is said that it might decompose

**Table 2** Comparison for material properties and effect on Soot mass limit

Substrate material	SC-AT	SiC	Cordierite	Effect on Soot mass limit
Theoretical density [g/cc]	3.7	3.2	2.6	High
Heat Capacity [J/L·K]	2000	1900	1300	High
CTE/ $\times 10^{-6}$ [1/K]	1	4	< 1	High
Thermal Conductivity [W/m·K]	2	50	2	Low

into titania and alumina. The DPF reaches a temperature in this range during PM regeneration, and this has been deemed as the greatest problem when using AT as a DPF material. Paying attention to this point as well, we have developed an AT material that can be prevented from thermal decomposition within this temperature range as well.<sup>5)</sup>

## 2. Pore Structure Design

DPF partition wall possesses a “pore structure” that consists of minute pores in the order of microns. This structure (i.e. pore size and distribution) greatly affects the filtration efficiency and pressure drop characteristics. This means that in order to efficiently collect PM, it is preferable that the porosity and pore diameter are as small as possible. Contrastingly, in order to reduce the pressure drop (= allow gas to flow efficiently), larger porosity and pore diameter are better. The optimal pore structure can be determined by taking both characteristics into account. We conducted pore structure optimization on DPF products already on the market, through a small-scale experiment using the filtration efficiency and pressure drop characteristics as parameters (Fig. 3). Fig. 3 shows the pore characteristics (porosity and mean pore diameter) of each product and the characteristics of the filtration efficiency. Fig. 3 also indicates the pressure drop characteristics using the value of Serial (A) as a standard. Additionally, Serial (A), Serial (B) and Serial (C) are DPF products obtained from the market. Of all those products, Serial (A) is made of the material that can be considered to be the most popular in the current global market.

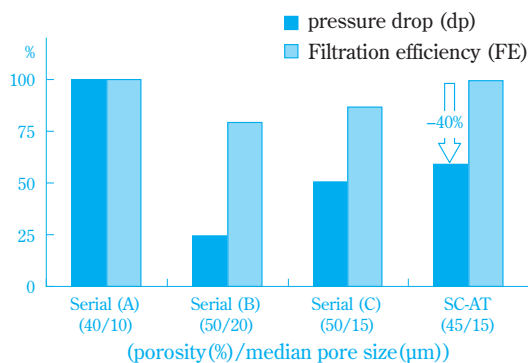


**Fig. 3** Filter performance on pressure drop (dp) and filtration efficiency (FE) for Serial filter and SC-AT under simulated experimental. dp and FE shows relative percentage for Serial (A).

Serial (A) possesses a partition wall which has relatively small pores (low porosity and small mean pore diameter). Therefore, it demonstrates extremely high filtration efficiency. Although Serial (B) and Serial (C) possess relatively large pores (high porosity and large mean pore diameter) and show lower pressure drop than Serial (A), they demonstrate low filtration efficiency. In order to achieve favorable pressure drop characteristics and filtration efficiency in a well-balanced manner, we have examined and improved the pore structure of SC-AT and discovered the structure that provides high filtration efficiency and low pressure drop.

## 3. Cell Structure Design

The filter cell structure is one of the most important design factors. (Fig. 4 shows an example of the cell structure of the on-market DPF product viewed from the inlet side. Fig. 5 also shows an image of the typical cell structure. The details are described later.)

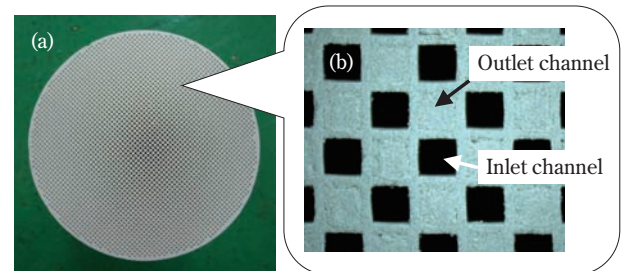


**Fig. 4** Photos in Cell geometry on filter structure (a) Inlet face on filter (b) An example of square (SQ) cell geometry.

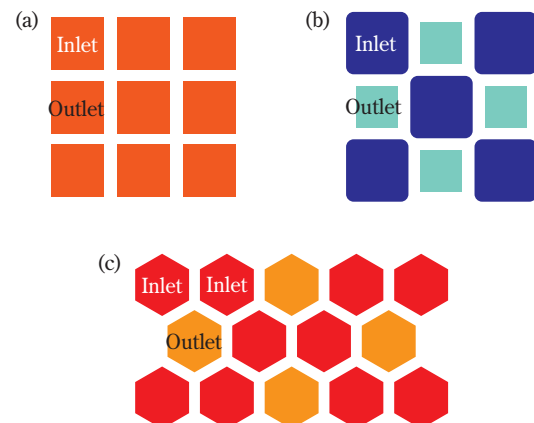


**Fig. 5** Variety in cell geometry. (a) Square design (SQ), (b) Octo-square design (OS), and (c) Hexahex design (HEX). Cell geometry consists of inlet and outlet channels.

One of the reasons for this is because the cell structure affects the filtration area, thus greatly influencing the DPF pressure drop characteristics. Another reason is that the cell structure significantly affects the ash-resistance characteristics, particularly the physical volume of ash accumulation (ash capacity).

### (1) Contribution of Cell Structure to Pressure Drop Characteristics

Pressure drop characteristics of DPFs are discussed under the following three states:

- (i) Bare (non-catalyzed state)
- (ii) Coated (catalyzed state)
- (iii) Life end (ash accumulation state)

In this study, the pressure drop characteristics of the DPFs were compared under the coated state (ii) in order to compare SC-AT to the “serial” DPFs (catalyzed products). (This state is equivalent to the default state when used for actual automobiles.)

The pressure drop characteristics of a DPF can be expressed by disassembling it into components as shown in equation (2).<sup>6)</sup> Subsequent to the PM accumulation, the pressure drop ( $dp_4$ ), which is equivalent to the resistance caused by the inflow gas passing through the PM accumulation layer, demonstrates the highest contribution ratio. Furthermore, “ $dp_4$ ” can be expressed using equation (3) and is substantially controlled by the height of the PM accumulation layer ( $w$ ).<sup>1, 3)</sup> By increasing the filtration area of a DPF, “ $w$ ” can be reduced in conditions where the amount of deposited PM is otherwise constant. It is therefore expected that the pressure drop characteristics of DPFs can be improved.

$$dp = dp_1 + dp_2 + dp_3 + dp_4 + dp_5 + dp_6 \quad (2)$$

$dp_{1, 6}$  ; expansion/reduction resistance inside the exhaust pipe  
 $dp_{2, 5}$  ; inlet- and outlet- channel through resistance  
 $dp_3$  ; wall material through resistance  
 $dp_4$  ; soot layer material through resistance

$$dp_4 = \mu u_s w/k_0 \quad (3)$$

$k_0$  ; constant for soot material  
 $\mu$  ; gas viscosity  
 $u_s$  ; gas velocity  
 $w$  ; thickness of soot layer on the wall

### (2) Contribution of Cell Structure to Ash Capacity

Solid components (other than PM) contained in

exhaust gas include non-organic components mixed in from the fuel and/or lubricating oil, as well as metal components mixed in due to the frictional wear of syringes. These solid components are collectively called ash components. Ash components gradually accumulate in the DPF, decreasing the effective filtration area, and can therefore cause an increase in pressure drop.

As a solution, other companies has proposed an asymmetrical cell structure in which the size of cells at the inlet side is larger than that of the cells at the outlet side (e.g., the OS cell structure (Octo-square)<sup>7)</sup>, the ACT cell structure (Asymmetric Cell Technology)<sup>8)</sup>. (Fig. 5 (b) shows the OS cell structure.) Because the OS cell structure has a larger open frontal area (OFA) than the conventional standard cell structure (Square; SQ, Fig. 5 (a)), it enables the ash capacity of a DPF to be increased. More specifically, it is said that the OS cell structure can increase the filter lifetime by approximately 30%.

### (3) Advantage of a HEX Cell Structure

In the OS cell structure the total cross-sectional area of the inlet cell channel and that of the outlet cell channel are imbalanced. Therefore, the structure has a disadvantage in that the gas flow becomes extremely rapid in one of the channels, thus increasing the channel resistance within the honeycomb and increasing the filter’s pressure drop (equivalent to the “ $dp_5$ ” component in equation (2)).

In contrast, the asymmetrical hexahex (HEX) that we have adopted (Fig. 5 (c)) is based on a unit consisting of several channels (usually two to three) with a small hydraulic diameter per channel (usually at the inlet side) for each single channel with a large hydraulic diameter (usually at the outlet side). Therefore, the total cross-sectional area of the inlet cell channels and that of the outlet cell channels can be designed to be equivalent, thereby suppressing the increase in channel resistance, which is a problem with the OS cell structure.<sup>9)</sup>

Furthermore, as described later in this paper, because the effective filtration area of the HEX cell structure is larger than that of the OS cell structure, it is expected that the pressure drop after PM accumulation can be reduced (because the height of the PM accumulation layer ( $w$ ) in equation (3) can be reduced due to the enlarged effective filtration area).

As described above, the HEX cell structure we have adopted can reduce the pressure drop and at the same time increase the ash capacity.



## Characterization

### 1. Comparing DPF Specifications

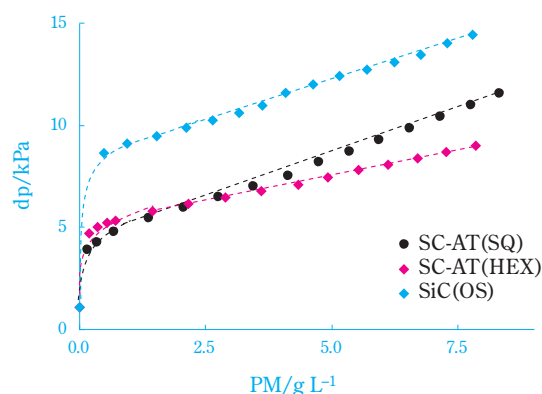
Combining all the specifications examined and developed during the material, pore and cell structure design processes, we made a standard size for DPF ( $\phi 5.66$  inch  $\times$  6.0 inch L) and conducted characterization tests to verify the validity of the above design concepts.

Two types of DPF having different cell structures (SQ, HEX) were made as the SC-AT models. Filter catalysis was outsourced and performed according to the prescriptions used for on-market DPFs. Furthermore, an on-market SiC (OS) DPF (currently incorporated in Euro 5-compliant automobiles) (equivalent to Serial (A) in Fig. 3) was used as a material comparison.

The DPF specifications are indicated in Table 3. Particularly for SC-AT (HEX), it can be observed that a large filtration area and a large OFA have been achieved. Moreover, the hydraulic diameters of the inlet and outlet cell channels were nearly equivalent with SC-AT (HEX), and therefore low pressure drop characteristics can be expected in addition to the ash capacity characteristics.

### 2. Pressure Drop Characteristics

Fig. 6 depicts the measurement results of the pressure drop characteristics during PM accumulation. The PM accumulation mode after passing the initial PM accumulation region (where the amount of deposited PM is less than 1g/L) is considered as the cake fil-

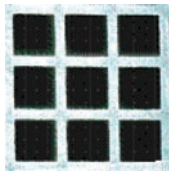
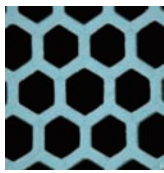
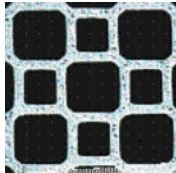


**Fig. 6** PM amount dependence on changes in pressure drop under cold flow bench. Filter dimension for all samples ; 5.66" in diameter and 6" in length with cylindrical shape.

tration region. In this region a linear increase in pressure drop, which occurred in proportion to the amount of deposited PM, was observed. This inclination was small for SC-AT (HEX) with a large filtration area, and thus the superiority in pressure drop characteristics of the HEX cell structure was confirmed.

Additionally, the initial PM accumulation region was referred to as the transient region. It is considered that in this region the PM infiltrate into the pores of the partition wall and accumulates in them. Regarding SiC (OS) having relatively small pores (= low porosity, small mean pore diameter), it was surmised that the pressure drop increased sharply because the pore channels tend to be occluded by PM. It was also confirmed that the pore characteristics of SC-AT advantageously affected the pressure drop characteristics.

**Table 3** Filter specification of validated filter samples

Filter	SC-AT		SiC
	Square (SQ)	Hexahex (HEX)	Octo-square (OS)
Cell geometry			
Weight [g L <sup>-1</sup> ]	800	800	700
Hydraulic diameter IN/OUT [mm]	1.2/1.2	1.2/1.3	1.5/0.9
Cell density [cps]	300	350	300
Wall thickness [mil]	12	11	11
Segment binding area [%]	–	–	5
Open frontal area [%]	33	41	44**
Filtration area [m <sup>2</sup> L <sup>-1</sup> ]	1.0	1.3	1.0**

\*\* Including frontal area loss by segment binding layer.

### 3. PM Collection Properties

The PM collection properties (filtration efficiency) were measured using a PM generator (REXS manufactured by Matter Engineering AG) and a particle counter (EEPS3090 manufactured by TSI). Also, in order to obtain a preparative gas in the measurement range that could detect the amount of PM, the gas was diluted first using a diluter (MD19-1i manufactured by Matter Engineering AG) and then introduced to the particle counter.

The filtration efficiency was obtained using the equation shown below, denoting the start time needed to allow the gas containing PM to flow into the DPF as  $t = 0$ s:

$$\text{Filtration efficiency (\%)} = 100 (1 - N_{600s}/N_0) \quad (4)$$

$N_0$  : The PM number concentration generated by the apparatus (number/cm<sup>3</sup>)

$N_{600s}$ : The PM number concentration passing through the DPF after 600s (number/cm<sup>3</sup>)

Fig. 7 shows the chronological change in the PM number concentration in the calculation of the filtration

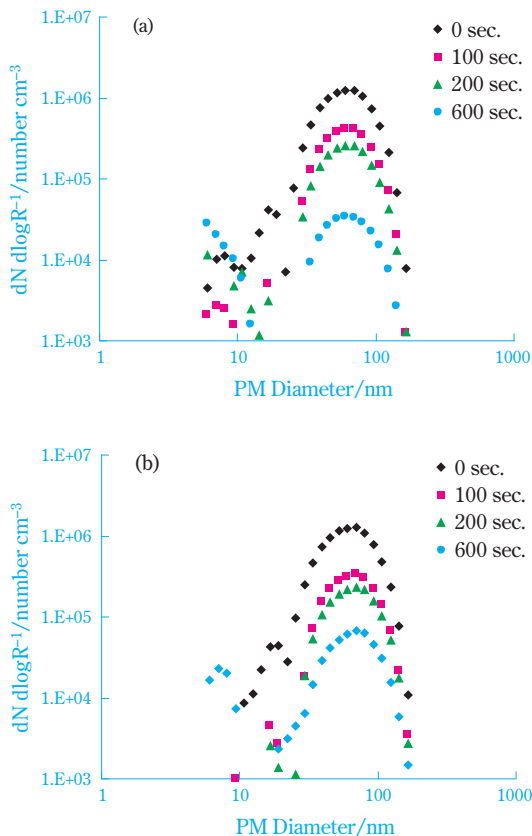


**Fig. 7** Changes in PM number distribution on downstream filter. (a) SC-AT(HEX) and (b) SiC(OS).

efficiency. For each DPF, the PM number concentration decreased chronologically for particles of any diameter, and the PM was efficiently filtered by the DPFs. When the filtration efficiency of each DPF was calculated using equation (4), the results were 96% for SC-AT (HEX) and 94% for SiC (OS), thus indicating that SC-AT (HEX) possessed a PM collection capability equivalent to or greater than that of SiC (OS).

### 4. SML (Soot Mass Limit) Test

Using an engine bench manufactured by a European evaluation institute, an SML test was conducted in order to investigate the thermal shock resistance of the DPFs. DPF regeneration was performed in drop-to-idle (hereinafter referred to as “DTI”) mode, also known as the worst-case regeneration, as described below:

#### (1) The System Used

A 2.0L-class DI engine (maximum horsepower: 110kW; maximum torque: 330Nm; common-rail fuel injection system) was used. A Diesel Oxidation Catalyst (DOC) was positioned upstream of the DPF. Also, during measurement a thermocouple (K-type) was set into the DPF from the downstream side of the DPF to monitor the temperature behavior during regeneration, as shown in Fig. 8. Additionally, Fig. 8 depicts the SML test flow and the typical temperature behavior by the thermocouple.

#### (2) Test Conditions (DTI)

First, a specified amount of PM was allowed to accumulate in the DPF. The amount of accumulated PM was confirmed by weighing the DPF after detaching it from the engine bench along with the canning case. After reinstalling the canning case to the engine bench, the engine was operated at a specified mode and then the temperature was increased to the point where the gas temperature reached 630°C at the DPF upstream through post injection (PIJ). Subsequently, the decrease in the differential pressure drop between the front of and the back of the DPF (= start of PM combustion) was detected, whereupon the engine was turned down to the idle condition. Table 4 shows the PIJ and idle engine operating conditions during SML test.

The reason DTI mode is referred to as worst-case regeneration is because, as shown in Table 4, the amount of gas rapidly decreases due to the transition to idle state, thus hindering the heat removal during

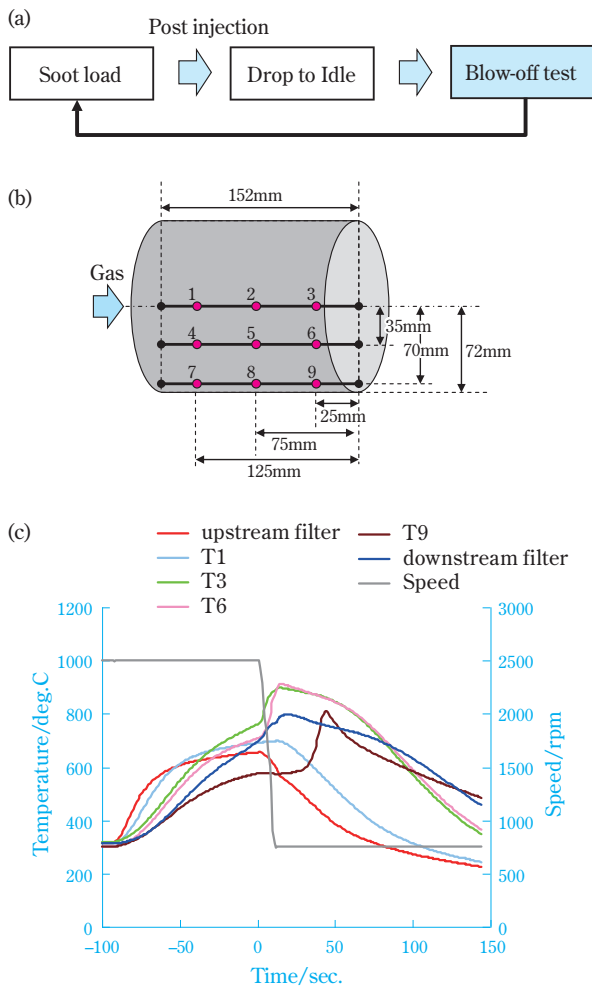


**Fig. 8** Image of SML test and an example of temperature behavior. (a) SML test procedure, (b) thermocouple position inside filter under SML test, and (c) an example of changes in engine rotation and temperature at individual position. 0 sec. in time on Fig.8 (c) indicates a start of DTI mode.

**Table 4** Condition of SML test (Post injection (PIJ) and Idle)

Engine condition	Speed	Gas flow rate	O <sub>2</sub> concentration
PIJ	2,500 rpm	230kg/h	8%
Idle	750 rpm	50kg/h	19%

the PM combustion and causing a runaway reaction. This is also propelled by the increased oxygen concentration.

In the SML test, the initial condition of the amount of accumulated PM was 8g/L (or 10g/L). Once the sample passed the test described below, the amount of deposited PM was further increased by 2g/L and then a similar SML test was conducted.

### (3) Blow-off Test

Subsequent to the SML test, a PM leakage test called a blow-off test (conducted by allowing the PM-contained gas upstream from the DPF to flow through the DPF in order to detect the amount of PM contained in the gas downstream of the DPF) was used to determine the presence of damage in the DPF due to the thermal shock upon PM combustion. The smoke limit in the blow-off test, as shown in Fig. 9, is an empirical value provided by an evaluation institute, which can be used as an indicator of DPF damage (i.e., if the value exceeds the smoke limit, it is judged that the DPF has been damaged).

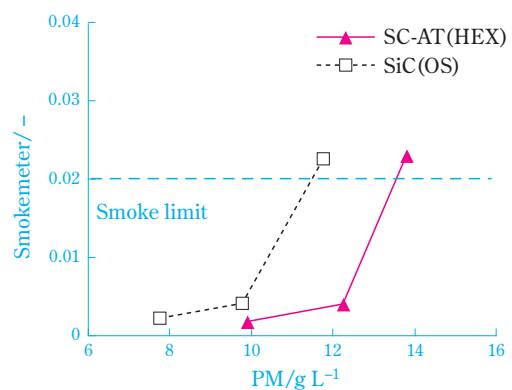


**Fig. 9** Blow-off test result after SML test as a function of PM amount on filter.

### (4) SML Test Results

The SML test was performed using SiC (OS) and SC-AT (HEX). Fig. 9 depicts the results of the blow-off test for the amount of accumulated PM conducted after the SML test. It was observed that SC-AT (HEX) demonstrated better thermal shock resistance characteristics than SiC (OS).

The regeneration efficiencies (i.e., how efficiently the PM was burned and removed) under various conditions were plotted using the accumulated PM amount as the evaluation criterion. As shown in Fig. 10, SC-AT (HEX) showed a PM regeneration efficiency which was equivalent to or greater than that of the on-market DPF. Furthermore, Fig. 11 depicts the mapping of the internal temperature of each DPF (a prediction of the temperature distribution in the DPF based on the temperature of the area between the thermocouples calculated using the thermocouple temperature data). (In Fig. 11 it was difficult to estimate the temperature distribution in the areas having a length of 5 inches or greater merely by calculation, because it was assumed that a



rapid temperature change might have occurred due to the generation heat.) It is said that PM combustion begins at a temperature of approximately 630°C. Therefore, it was predicted that PM combustion would progress over a wide area of the SC-AT (HEX) because this type of DPF has a large area with a temperature exceeding 630°C.

Furthermore, as a result of another investigation regarding the effects of the cell structures using the same AT material, the following findings were confirmed: According to the results of a SML test conducted under the same PM accumulation conditions, the maximum internal temperature of the HEX structure was lower than that of the SQ structure, indicating that the HEX structure suppressed the temperature increase during PM combustion (= mild regeneration).

Because mild combustion of PM in a broad area was achieved with SC-AT (HEX), we believe the thermal

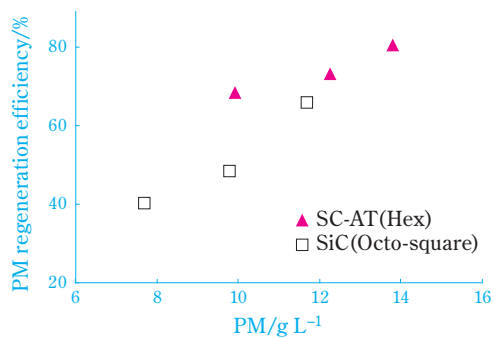


**Fig. 10** PM regeneration efficiency as a function of PM amount on filter.

shock resistance and regeneration efficiency have been successfully improved.

Currently, the causes of the mild regeneration in SC-AT (HEX) are under investigation.

#### (5) Effects of Cyclic Regeneration

A cyclic regeneration test was conducted on SC-AT (SQ) in DTI mode. The amount of deposited PM used for the test was 8g/L×5 times and 10g/L×5 times. As seen in the results of the blow-off test shown in Fig. 12, the smoke meter values were consistently low, indicating that even after cyclic regeneration, no damage to the DPF was incurred. It was therefore predicted that cyclic regeneration would not cause any problems during practical use.

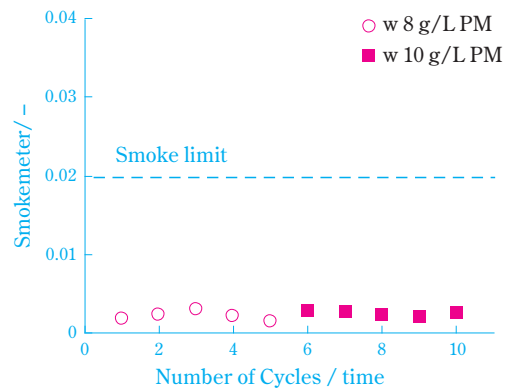


**Fig. 12** Blow-off test results for SC-AT (SQ) after Cyclic regeneration with 8 and 10 g/L PM amount.

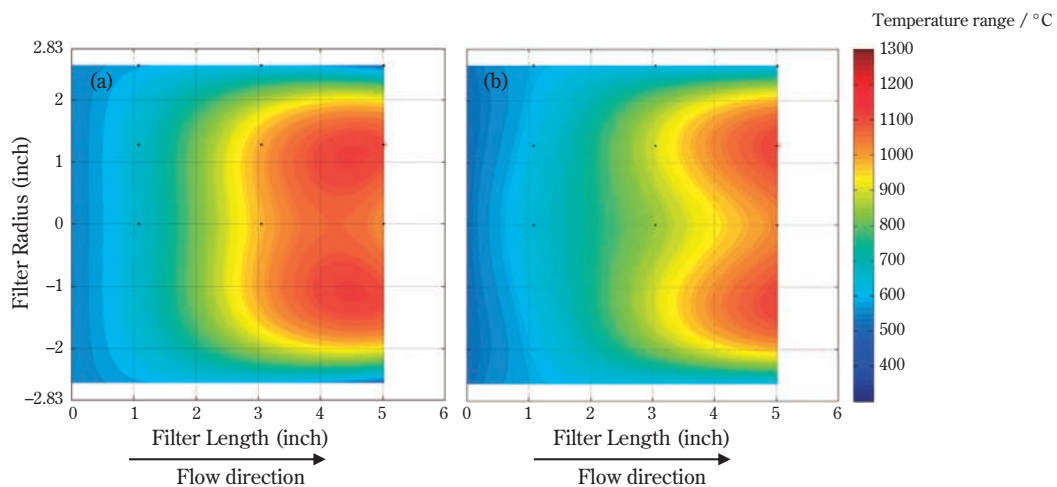


**Fig. 11** Temperature distribution inside filter (5.66" diam. and 6" length) at maximum temperature on (a) SC-AT(Hex) and (b) SiC(OS). PM amount on filter is 12g/L. Exhaust gas flows from left side to right side in the figure.

## Conclusion

In this paper we have introduced a DPF design concept, as well as the validation of the product design through the characterization of a newly created DPF based on the above-described design concept.

Compared to the on-market DPFs, the DPF developed by Sumitomo Chemical demonstrated lower pressure drop, higher filtration efficiency and higher thermal shock resistance, thereby proving the validity of the product design. We believe these characteristics were achieved through the combination of our outstanding material design (the development of an AT having low thermal expansion properties and high thermal stability), pore design (achieved by optimizing the pore-forming material and production conditions) and furthermore, an intelligent cell design (adoption of a HEX structure that provides a large filtration area and milder temperature increase upon DPF regeneration).

Regarding the product design validation, only the items referred to as the initial characteristics were introduced in this paper. However, in order to load the new DPF in diesel-powered automobiles it is desirable to verify the following items: the effect of highly reactive inorganic components having accumulative properties (ash components) that can mix in the filter from the fuel or the environment; the effect of mechanical vibrations; and the overall long-term durability characteristics. Regarding the evaluation of those characteristics, tests are being conducted in cooperation with external evaluation organizations.

Moreover, in response to enhanced legal restrictions, we are continuing to develop the DPF technology introduced in this paper and are expanding its applications to new fields. These activities include the development of a new GPF (Gasoline Particulate Filter) for gasoline-powered automobiles<sup>10)</sup> (compliant with the Euro6 PM number restriction) and the incorporation with SCR (Selective Catalytic Reaction), which is one of the

measures for the enhanced NO<sub>x</sub> regulation<sup>11)</sup>, into DPFs.

As we aim for an early market launch of the DPF thus developed, we will continue to conduct various types of characterizations while brushing up our design, evaluation and analysis techniques for the newly created DPF in order to develop new products.

## References

- 1) K. Ohno, K. Shimato, N. Taoka, H. Santae, T. Ninomiya, T. Komori and O. Salvat, *SAE Technical Paper*, 2000-01-0185 (2000).
- 2) T. V. Johnson, *SAE Technical Paper*, 2008-01-0069 (2008).
- 3) K. Ohno, Doctoral dissertation at Waseda Univ., 2006
- 4) R. S. Ingram-Ogunwumi, Q. Dong, T. A. Murrin, R. Y. Bhargava, J. L. Warkins and A. K. Heibel, *SAE Technical Paper*, 2007-01-0656 (2007).
- 5) T. Fukuda, Masahiro Fukuda and Masaaki Fukuda, JPN Kokai Tokkyo Koho 2004-026508 (2004).
- 6) A. G. Konstandopoulos, *SAE Technical Paper*, 2003-01-0846 (2003).
- 7) K. Ogyu, K. Ohno, S. Hong and T. Komori, *SAE Technical Paper*, 2004-01-0949 (2004).
- 8) D. M. Young, D. L. Hickman, G. Bhatia and N. Gunasekaran, *SAE Technical Paper*, 2004-01-0948 (2004).
- 9) ROBERT BOSCH GMBH, JPN Kohyo Tokkyo Koho 2009-537741 (2009).
- 10) C. Saito, T. Nakatani, Y. Miyairi, K. Yuuki, M. Makino, H. Kurachi, W. Heuss, T. Kuki, Y. Furuta, P. Kattouah and C-D. Vogt, *SAE Technical Paper*, 2011-01-0814 (2011).
- 11) M. Naseri, S. Chatterjee, M. Castagnola, H.Y. Chen, J. Fedeyko, H. Hess and J. Li, *SAE Technical Paper*, 2011-01-1312 (2011).

## PROFILE

*Akiyoshi NEMOTO*

Sumitomo Chemical Co., Ltd.  
Basic Chemicals Research Laboratory  
Senior Research Associate

*Kousuke UOE*

Sumitomo Chemical Co., Ltd.  
Basic Chemicals Research Laboratory  
Senior Research Associate  
Doctor of Engineering

*Kentaro IWASAKI*

Sumitomo Chemical Co., Ltd.  
Basic Chemicals Research Laboratory  
Research Associate  
Doctor of Environmental Earth Science

*Tetsuro TOMA*

Sumitomo Chemical Co., Ltd.  
Basic Chemicals Research Laboratory  
Research Associate  
Doctor of Engineering

*Osamu YAMANISHI*

Sumitomo Chemical Co., Ltd.  
Basic Chemicals Research Laboratory  
Senior Research Specialist

*Hajime YOSHINO*

Sumitomo Chemical Co., Ltd.  
Basic Chemicals Research Laboratory  
Researcher

*Kazuya TSUCHIMOTO*

Sumitomo Chemical Co., Ltd.  
Basic Chemicals Research Laboratory  
Senior Research Associate